frontiers | Frontiers in Ecology and Evolution

TYPE Original Research
PUBLISHED 20 October 2022
DOI 10.3389/fevo.2022.969158

OPEN ACCESS

EDITED BY
Tae-Yoon Park,
Korea Polar Research Institute,
South Korea

REVIEWED BY
John Albert Long,
Flinders University, Australia
Zerina Johanson,
Natural History Museum,
United Kingdom

*CORRESPONDENCE
Melina Jobbins
melina.jobbins@pim.uzh.ch

SPECIALTY SECTION
This article was submitted to Paleontology, a section of the journal Frontiers in Ecology and Evolution

RECEIVED 14 June 2022
ACCEPTED 23 September 2022
PUBLISHED 20 October 2022

CITATION
Jobbins M, Rücklin M, Ferrón HG and Klug C (2022) A new selenosteid placoderm from the Late Devonian of the eastern Anti-Atlas (Morocco) with preserved body outline and its ecomorphology. *Front. Ecol. Evol.* 10:969158. doi: 10.3389/fevo.2022.969158

A new selenosteid placoderm from the Late Devonian of the eastern Anti-Atlas (Morocco) with preserved body outline and its ecomorphology

Melina Jobbins[1]*, Martin Rücklin[2,3], Humberto G. Ferrón[4,5] and Christian Klug[1]

[1]Palaeontological Institute and Museum, University of Zurich, Zürich, Switzerland, [2]Naturalis Biodiversity Center, Leiden, Netherlands, [3]Sylvius Laboratory, Institute of Biology, University of Leiden, Leiden, Netherlands, [4]Instituto Cavanilles de Biodiversidad y Biología Evolutiva, Paterna, Spain, [5]School of Earth Sciences, University of Bristol, Bristol, United Kingdom

Placoderms are an extinct group of early jawed vertebrates that play a key role in understanding the evolution of the gnathostome body plan, including the origin of novelties such as jaws, teeth, and pelvic fins. As placoderms have a poorly ossified axial skeleton, preservation of the mainly cartilaginous axial and fin elements is extremely rare, contrary to the heavily mineralized bones of the skull and thoracic armor. Therefore, the gross anatomy of the animals and body shape is only known from a few taxa, and reconstructions of the swimming function and ecology are speculative. Here, we describe articulated specimens preserving skull roofs, shoulder girdles, most fins, and body outlines of a newly derived arthrodire. Specimens of the selenosteid *Amazichthys trinajsticae* gen. et sp. nov. display a skull roof with reticular ornamentation and raised sensory lines like *Driscollaspis*, a median dorsal plate with a unique sharp posterior depression, the pelvic girdle, the proportions and shape of the pectoral, dorsal, and caudal fins as well as a laterally enlarged region resembling the lateral keel of a few modern sharks and bony fishes. Our new phylogenetic analyses support the monophyly of the selenosteid family and place the new genus in a clade with *Melanosteus*, *Enseosteus*, *Walterosteus,* and *Draconichthys*. The shape of its body and heterocercal caudal fin in combination with the pronounced "lateral keel" suggest *Amazichthys trinajsticae* was an active macropelagic swimmer capable of reaching high swimming speeds.

KEYWORDS

Selenosteidae, body outline, Morocco, Famennian, geometric morphometrics

Introduction

Placoderms play a key role in the early evolution of jawed fish (Jarvik, 1980; Reif, 1982; Janvier, 1984; Young, 1986, 2010; Forey and Janvier, 1993; Philippe, 1996; Donoghue et al., 2000; Sansom et al., 2005; Anderson et al., 2011; Kuratani, 2012; Zhu et al., 2013, 2021; Brazeau and Friedman, 2014, 2015; Giles et al., 2015; King et al., 2017). In particular, the origins of jaw elements and teeth were intensely studied in the past decades through the Placodermi group (Smith and Johanson, 2003; Rücklin et al., 2012, 2014; Zhu et al., 2013, 2016; Coatham et al., 2020; Vaškaninová et al., 2020; Jobbins et al., 2021). Complete skeletons of some representatives of placoderm clades, such as the Antiarchi (Long, 1983; Johanson, 1997), Petalichthyida (Gross, 1961), and Ptyctodontida (Ørvig, 1960), are found more commonly, sometimes even including soft parts (Gardiner, 1984; Young, 1986; Long et al., 2008). By contrast, skeletons of Arthrodira are hardly known (Miles and Westoll, 1968; Ahlberg et al., 2009; Carr et al., 2009, 2010; Long et al., 2009; Trinajstic et al., 2015; Gess and Trinajstic, 2017; Rücklin et al., 2018). Consequently, complete skeletons of arthrodires are of great interest because of their potential to reveal unknown aspects of their anatomy, including overall proportions, form, and size of the fins, the structure of the integument, and internal organs as far as they are preserved.

Accordingly, the complete skeletons of a medium-sized arthrodire species from the Late Devonian of the Moroccan Anti-Atlas yield valuable information on various anatomical details. Here, we introduce the new taxon *Amazichthys trinajsticae* gen. et sp. nov. The type material comprises six specimens, one skull roof, and four more or less well-preserved skeletons of the early to middle Famennian age. We document its anatomy and discuss its phylogenetic position within selenosteids. Moreover, the exceptional preservation of two of these skeletons enables us to discuss the functional morphology of the fins and body outline and to hypothesize about swimming capabilities.

Materials and methods

All specimens were found in the southern part of two small epicontinental basins, namely the Tafilalt Basin in the east and Maïder Basin in the west of the eastern Anti-Atlas (Wendt, 1985, 1988, 2021). Late Devonian strata in the Anti-Atlas yield many fossiliferous layers containing abundant vertebrates and invertebrates. All the skeletons described here were extracted from the Thylacocephalan Layer. This layer is named after its high abundance of thylacocephalan arthropods (Frey et al., 2019b; Jobbins et al., 2020) and dates back to the Middle Famennian *Maeneceras* genozone (Becker et al., 2002). It crops out at various localities in the southern Maïder (Frey et al., 2018; **Figure 1**). The skull roof is the only specimen that was not found in the Thylacocephalan Layer, but was found in Jebel Ouaoufilal, in the Southern Tafilalt, and is of Famennian age.

In total, three specimens, including two with almost completely preserved body outlines were excavated by Saïd Oukherbouch. An additional one was found by Saïd but the plates were indistinguishable and thus were not used in the study (AA.MEM.DS.11). Two specimens, one collapsed skull and shoulder girdle and the skull roof, were collected by Moha Mezane. The holotype AA.MEM.DS.8 comes from Rich Bou Kourazia (**Figure 1**). PIMUZ A/I 4773, wrongly numbered as PIMUZ 36882 in Frey et al. (2019b), was collected at Rich Bel Ras. AA.MEM.DS.10 was recovered from the Khrabis locality. The skull roof, PIMUZ A/I 5141, was collected at Jebel Ouaoufilal, an outcrop from the Famennian layer in the Tafilalt. PIMUZ A/I 5140 and AA.MEM.DS.9 were collected at Madene El Mrakib. The specimens are registered in the collections of the Palaeontological Institute and Museum of the University of Zurich, Switzerland (PIMUZ numbers) and at the Université Cadi Ayyad, Faculté des sciences et techniques, Département des sciences de la terre, Laboratoire Géosciences et Environnement in Marrakech (AA.MEM.DS. numbers), Morocco.

Taphonomy and preservation

The isolated skull roof PIMUZ A/I 5141 is preserved three-dimensionally as an only slightly compressed element in limestone. All other specimens are preserved, mostly as external molds, in large flat nodules like the chondrichthyans from the same strata and region (Frey et al., 2018, 2019a,b, 2020). The skeletons are partially embedded, lying in and on large ironstone nodules, which correspond roughly to the outline of the carcass. We assume that, during decay, organic matter seeping into the sediment changed the chemical composition and particularly the pH in such a way that it fostered the formation of very early diagenetic pyrite (Frey et al., 2019b). Due to weathering, this pyrite later became oxidized to hematite, limonite, and other iron minerals, hence the reddish to yellowish colors. In some parts, more or less concentric ridges surrounding the fossils document mineralization fronts (Frey et al., 2019b; Klug et al., 2021). Importantly, this taphonomic and diagenetic history enabled the preservation of the body outline including pectoral, dorsal, and caudal fins. Although not comparable to the preservation of placoderms from the Frasnian Gogo-Formation of Australia (Ahlberg et al., 2009; Long et al., 2009, 2015; Trinajstic et al., 2015, 2022), this concretionary skin outline-preservation is unique in its kind. Body outlines are also known from, e.g., Early Jurassic ichthyosaurs, but their taphonomic history is different because the outlines represent the phosphatized cutis (Lindgren et al., 2018).

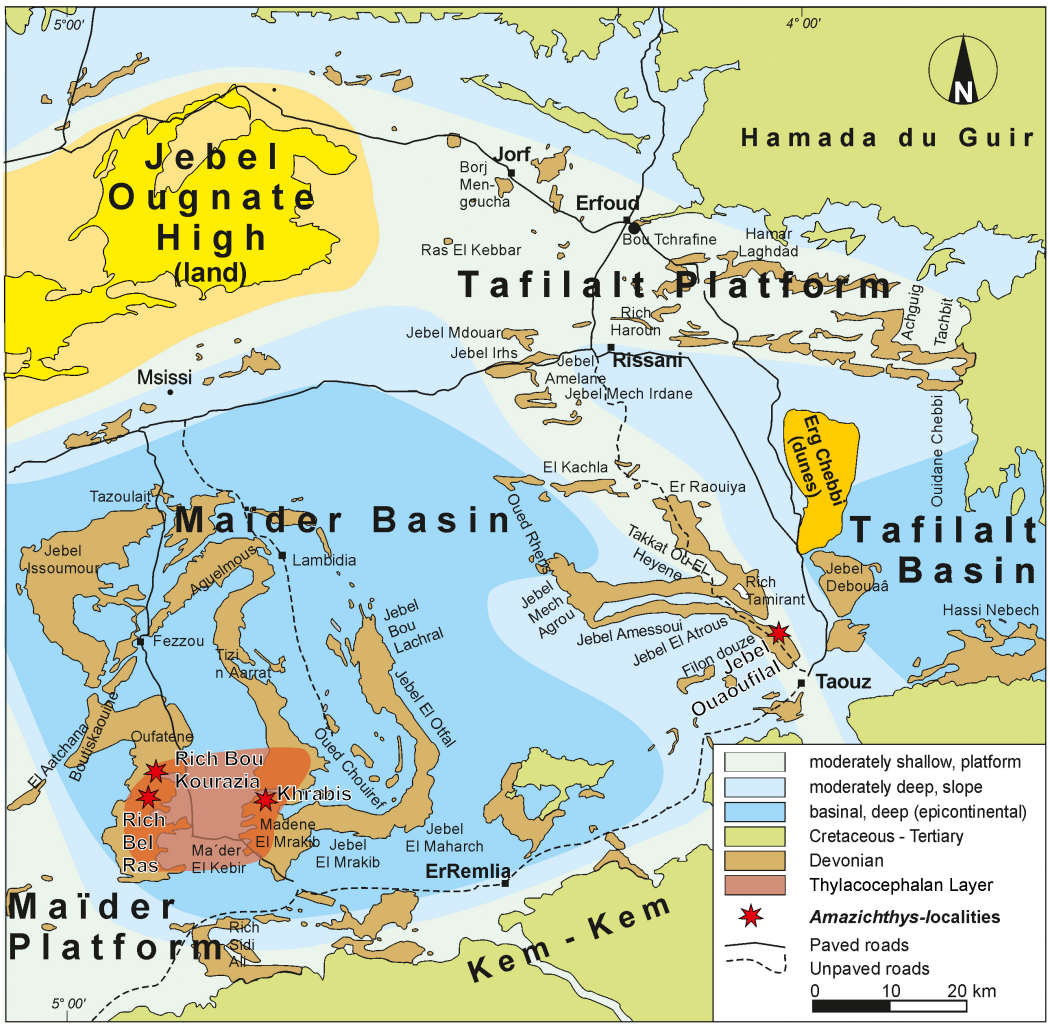

FIGURE 1
Map of the Anti-Atlas with the localities where *Amazichthys trinajsticae* gen. et sp. nov. specimens were collected.

Fossil preparation and casting positives

Very little mechanical preparation was required for most of the specimens, where thin layers of clays coated parts of the skeleton. PIMUZ A/I 5140 and AA.MEM.DS.9 were subject to some preparation using the sandblaster. Merle Greif and Beat Scheffold made silicon casts of the head and thoracic armor of AA.MEM.DS.8, its pelvic girdle, and scapulocoracoids of PIMUZ A/I 4773 and AA.MEM.DS.10.

Photography, digital tomography, and segmentation

Photographs of each specimen, their structures, and their negatives were taken with a Nikon D2X. Pictures were processed (grayscale, levels, removing background, and inverting the positives to have the same direction as the negative) for the figures using Adobe Photoshop, Gimp, and Affinity Designer. **Figure 1** was produced using CorelDraw. AA.MEM.DS.11 was CT scanned at Qualitech in Mägenwil, Switzerland. The specimen was then segmented using the Mimics v19 software. Virtual thin sections, segmentation, and 3D model reconstructions were used to attempt to reconstruct the plates of AA.MEM.DS.11.

Phylogenetic analysis

The character matrix is based on Rücklin et al. (2015). It contains 98 characters; a few coding errors were corrected. The 28 taxa matrix was converted into a nexus file using Mesquite (Maddison and Maddison, 2021) and processed in PAUP (Swofford, 2003). The list of changes, along with the matrix, are available in the **Supplementary material**.

Morphometric analysis of ecomorphotypes

For comparison with *Amazichthys*, the morphological diversity of body and caudal fin outlines of 472 different species of extant sharks were assessed using a contour analysis (Elliptic Fourier analysis, EFA) and geometric morphometrics (GM). Body outlines (excluding the paired, anal, and dorsal fins) were digitized using TpsDig v.2.26 (Rohlf, 2016) based on lateral-view illustrations of sharks from Ebert et al. (2013). EFA was then carried out in the "Momocs" v.1.3.2 package (Bonhomme et al., 2014) in R (R Core Team, 2020) considering a total number of 25 harmonics, which gather nearly 99% of the cumulative harmonic power (**Supplementary Figure 2**) and reconstructs actual morphologies with high accuracy (**Supplementary Figure 3**).

Landmark digitization for the GM analysis was also performed on lateral-view illustrations of sharks from Ebert et al. (2013) using TpsDig v.2.26 (Rohlf, 2016). Our landmark configuration included a total of two landmarks of type I (placed on the lowest point on the dorsal border and the highest point on the ventral border of the caudal peduncle) and 148 landmarks of type III that were equally interpolated along the caudal fin outline. Generalized Procrustes analysis (GPA) was performed in the "Geomorph" v.4.1.2 R package (Adams et al., 2016) to remove the variation in translation, rotation, and size from the original landmark configurations. No sliding methods for Type III landmarks were implemented.

We derived two virtual morphospaces by performing a principal component analysis (PCA) on the Fourier harmonic coefficients (for the body outlines) using the "stats" v.4.1.1 R package and on Procrustes shape coordinates (for the caudal fin outlines) using the "Geomorph" v.4.1.2 R package (Adams et al., 2016), where actual specimens were plotted and colored by ecomorphotypes using the "ggplot2" v.3.3.5 R package (Wickham, 2016). Considered ecomorphotypes include macropelagic (i.e., large-sized pelagic species), littoral pelagic (i.e., generalized feeders and swimmers), benthic (i.e., slow swimming dermersal and benthic species), and bathic and micropelagic (i.e., slow swimming deep water species), which relate to Groups I–IV, respectively, in the well-established categorization of Thomson and Simanek (1977). We further calculated average Euclidean distances between *Amazichthys* and the different ecomorphotypes using the "stats" v.4.1.1 R package. R code and associated files are available in the Electronic **Supplementary material**.

Abbreviations

Institutional Abbreviation—PIMUZ, Palaeontological Institute and Museum, University of Zurich, Zurich, Switzerland. AA.MEM.DS., Université Cadi Ayyad, Faculté des sciences et techniques, Département des sciences de la terre, Laboratoire Géosciences et Environnement in Marrakech.

Systematic paleontology

PLACODERMI McCoy, 1848
ARTHRODIRA Woodward, 1891
SELENOSTEIDAE Dean, 1901b
AMAZICHTHYS gen. nov.

Type and only species included

Amazichthys trinajsticae, new species.

Etymology

Named after the North African ethnic group Amazigh (Berber), because the new taxon comes from their land.

Diagnosis

Same as type species.

AMAZICHTHYS TRINAJSTICAE sp. nov.

Etymology

Named after Kate Trinajstic (Perth, Australia), who has contributed greatly to early vertebrate research.

Diagnosis

Plates with reticular ridges forming the ornamentation and raised sensory lines. The anterior edge of the pineal plate occurs anterior to the orbit. Median dorsal plate with a depression at the posterior margin. Marginal plates are in contact with central plates. Junction of the postorbital, marginal, and central plates occurs posterior to the anterior margin of the nuchal plate. The dorsal fin is longer than high with a rounded posterior margin and begins nearly to the posterior end of the median dorsal plate. Pectoral fins share the approximate length of the dorsal fin but are shorter with a broadly rounded tip. The caudal fin has a dorsal lobe longer than the ventral lobe.

Differential diagnosis

The new genus differs from *Stenosteus*, *Gorgonichthys*, *Heintzichthys*, *Gymnotrachelus*, *Rhinosteus*, *Selenosteus*, *Melanosteus*, *Walterosteus,* and *Draconichthys* in the shallow preorbital plate embayment. In contrast to *Rhinosteus*, *Driscollaspis*, *Melanosteus*, *Enseosteus,* and *Draconichthys*, it has preorbital plates, which are separated by the rostral and pineal. The marginal plate of *Amazichthys* n. gen. does not form part of the orbit unlike what is observed in *Stenosteus*, *Rhinosteus*, *Selenosteus*, *Melanosteus*, *Walterosteus*, *Enseosteus,* and *Draconichthys*. The angle between the postorbital and otic branches of the infraorbital sensory line is between 45 and 90°, which is different than in *Stenosteus*, *Gymnotrachelus*, *Rhinosteus*, *Walterosteus,* and *Enseosteus*.

Age

Maeneceras genozone, Thylacocephalan Layer, middle Famennian, and Late Devonian.

Localities

Jebel Aoufilal, Rich Bou Kourazia, Rich Bel Ras, Madene El Mrakib, and Khrabis (Eastern Anti-Atlas, Morocco).

Holotype

AA.MEM.DS.8 is an almost complete skeleton with the external mold of the skull roof and partial inferognathal, near complete thoracic armor, pelvic girdle, with remains of the vertebral column, a laterally enlarged region similar to a shark's lateral keel anterior to the caudal fin of some recent chondrichthyans or teleosts, and a preserved body outline, which displays the dorsal, pectoral, and caudal fins.

Paratypes

PIMUZ A/I 5141, a near complete well-preserved skull roof, possibly lacking the rostral plate. PIMUZ A/I 4773 comprises the external mold of a thoracic armor, scapulocoracoid, laterally enlarged region similar to a shark's lateral keel, remains of the vertebral column, and some of the body outline including a portion of the dorsal fin and a collapsed caudal fin. PIMUZ A/I 5140 is a partial skeleton including an inferognathal and the external mold of the thoracic armor and scapulocoracoid. AA.MEM.DS.9 comprises both inferognathals, a partial thoracic armor, a section of the scapulocoracoid with radials, and some traces of vertebral elements. AA.MEM.DS.10 includes the mold of a partially complete thoracic armor, scapulocoracoid, and some vertebral remains. AA.MEM.DS.11 is a partially preserved collapsed skull roof and thoracic armor.

Remarks

The skull roof of the holotype shares most characters with that of PIMUZ A/I 5141, the only specimen from the Tafilalt, in its stratigraphical position, morphological features, and ornamentation, indicating that both are from the same species. The thoracic armor of the other specimens corresponds well with that of the holotype, thus meaning they are conspecific. Individual descriptions of each specimen are available in the **Supplementary material**.

Description

Body form and proportions

AA.MEM.DS.8 and A/I 4773 preserve the body outline of the animal, including some of the fins (**Figure 2**). AA.MEM.DS.8 is the most complete specimen and is 87 cm long and 34 cm high dorsoventrally (**Figures 2A,B**). It consists of the external mold of the skull roof and an inferognathal, the left side of the thoracic armor, both posterior ventrolateral plates, the left pelvic girdle, and remnants of the left scapulocoracoid and axial skeleton. It also presents the impressions of both pectoral fins, a dorsal fin, and the caudal fin with a laterally enlarged region apparent to a shark's lateral keel (Bernal et al., 2001; Donley et al., 2004; Shadwick, 2005) reaching from slightly behind the pelvic girdle to the base of the caudal fin. There is neither an anal fin nor posterior dorsal fin apparent.

PIMUZ A/I 4773 is 77 cm long and 33 cm high from the top of the dorsal fin remains to the ventral margin of the ventrolateral plates (**Figures 2C,D**). It comprises the external mold of the left side of the thoracic armor, the left scapulocoracoid, and the caudal fin. It also presents portions of the axial skeleton and possibly the dorsal fin. A "lateral keel" is visible, reaching from slightly posterior to the pelvic girdle to the base of the caudal fin.

Skull roof

The skull roof is best preserved in PIMUZ A/I 5141 (**Figure 3**). It is 119 mm long and 124 mm wide. All skull measurements were taken from this specimen and are provided in **Table 1**. All of the preserved plates display a tubular ornament forming reticular ridges, which are about 1 mm wide. Toward the sutures, the ornament weakens. Sensory lines are bordered by elevated ridges. The posterior margin is gently concave and the skull roof tapers anteriorly. The rostral plate is not preserved but the specimen suggests that it would have been in direct contact with the pineal plate, separating the left and right preorbital plates. The pineal plate is large, it occupies about two-thirds of the area the preorbital does. It has a straight anterior margin located anterior to the orbit and a "V"-shaped posterior margin where it meets the central plates. A pineal foramen is present near the center of the plate. The preorbital plates are anteriorly concave, with jagged pineal and central contact margins. The sensory lines form a furrow between elevated bony ridges, which are about 1 mm wide (**Figure 4**). The supraorbital sensory line crosses the surface of the plate and rests above the dermal ornamentation (**Figures 4A,B**). The postorbital plates are "D"-shaped and have a medium-sized postorbital process. The postorbital plates are longer than the preorbital ones. Three sensory-line grooves meet at its center of ossification. The central sensory line curves posteriorly before splitting into the otic and postorbital branches of the infraorbital canal at a near 45° angle. The marginal plates are sub-rectangular and have short contact with the central plates. The post-marginal canal meets the otic branch of the infraorbital and the main lateral line on the surface of the marginal plate, the meeting point is preserved in PIMUZ A/I 5140 (**Figure 4C**). The central plates constitute the largest plates of the skull roof. Their lateral margin possesses two well-defined lobes, one at the anterior and one at the posterior end. The supraorbital sensory line is well-defined, but the central sensory-line canal is not. PIMUZ A/I 5141 presents short middle pit lines near the center of the plates. The paired central plates interlock with one another. The nuchal plate is triangular in a dorsal view with a concave posterior margin. The median process and a small right posterior section are not preserved. The nuchal plate is the second largest plate of the skull roof, it is deeply emarginated posteriorly and its anterior margin extends as two small lobes on each side forming

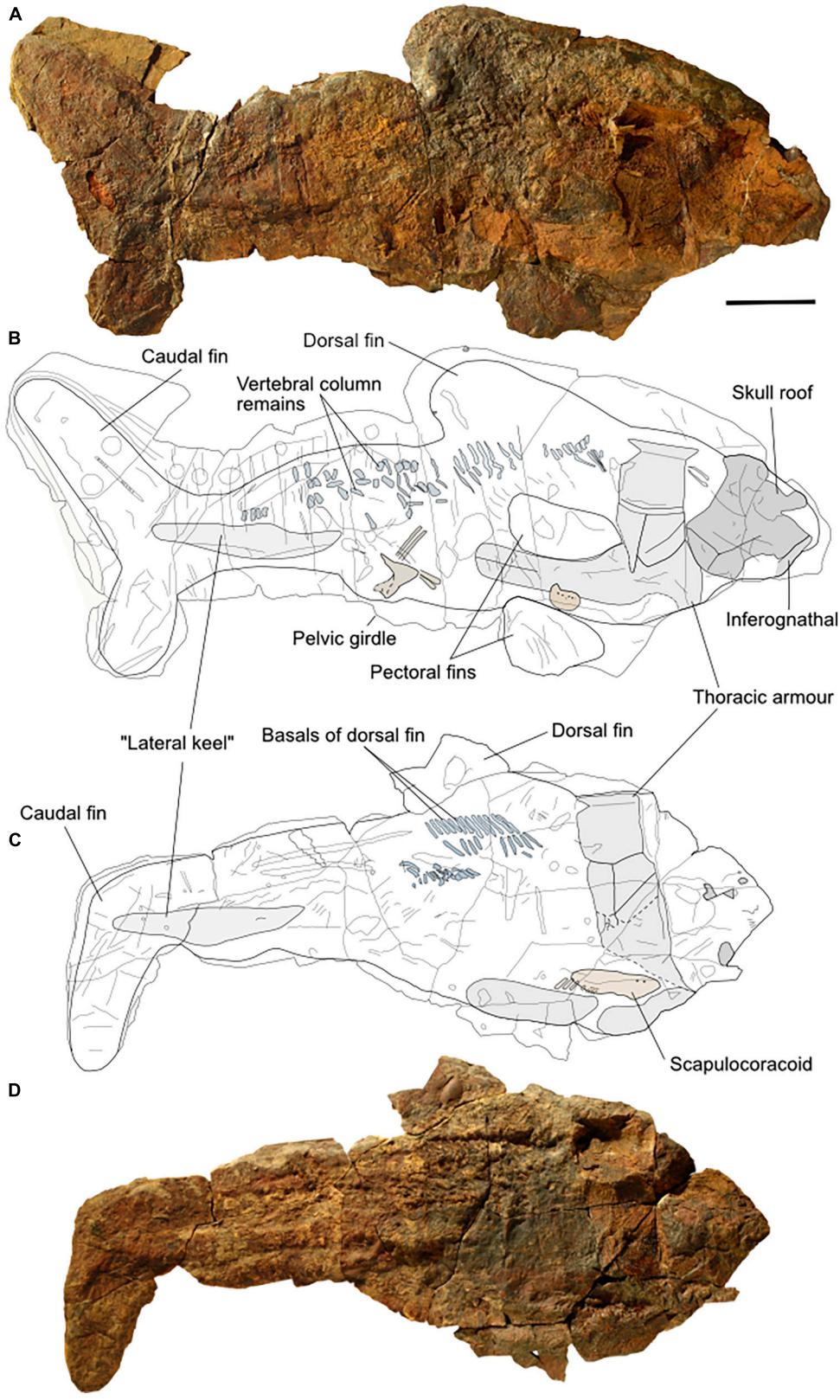

FIGURE 2
Two main specimens of *Amazichthys trinajsticae* gen. et sp. nov. The holotype, AA.MEM.DS.8 **(A)**, and its line drawing **(B)**, and PIMUZ A/I 4773 and its line drawing **(C,D)**. The scale bar corresponds to 100 mm.

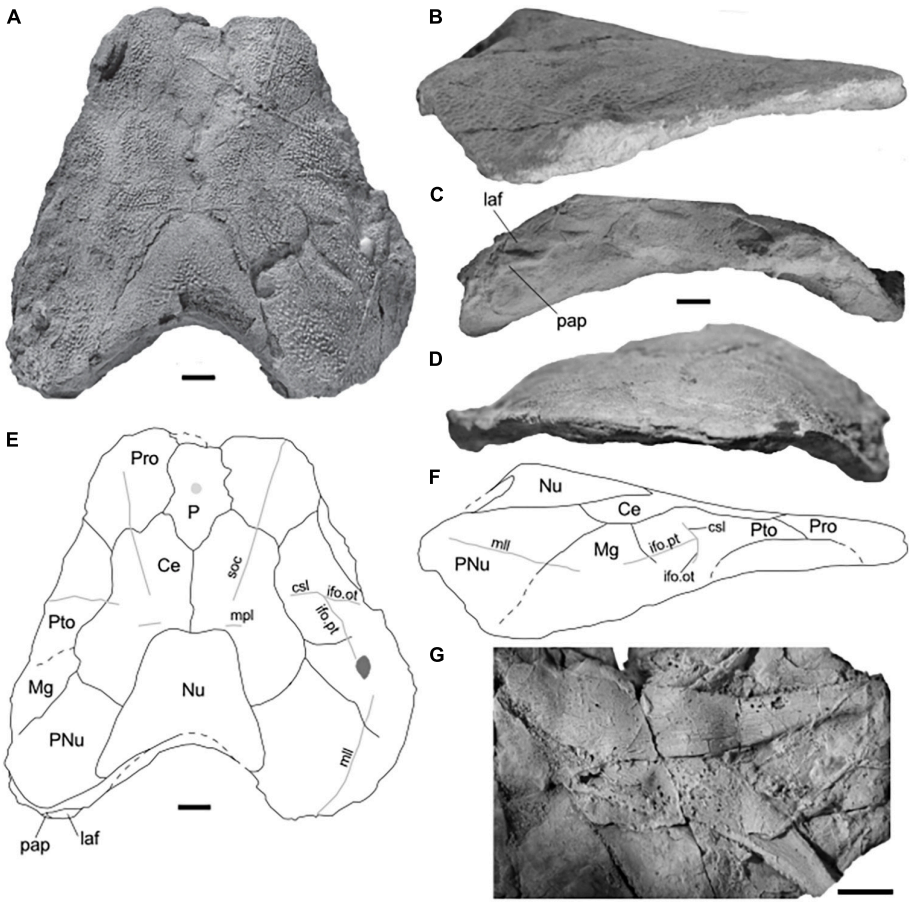

FIGURE 3
Skull roof and lower jaw of *Amazichthys trinajsticae* gen. et sp. nov. **(A–F)** PIMUZ A/I 5141 in dorsal **(A)**, lateral **(B)**, posterior **(C)**, and frontal view **(D)**. Line drawing of dorsal **(E)** and lateral-view **(F)**. **(G)** Nearly complete lower jaws from AA.MEM.DS.9 **(G)**. Scale bars correspond to 10 mm. Ce, central plate; csl, central sensory line canal; ifo.ot, otic branch of the infraorbital sensory line canal; ifo.pt, postorbital branch of the infraorbital sensory line canal; laf, lateral articular fossa; Mg, marginal plate; mll, main lateral line canal; mpl, middle pit line; Nu, nuchal plate; P, pineal plate; pap, para articular process; PNu, paranuchal plate; Pro, preorbital plate; Pto, postorbital plate.

an "M" shape. The paired paranuchal plates are a little bit wider than the preorbital plates and shorter than the central plates. The main lateral line crosses the dorsal surface from the anterior margin to the posterior end of the paranuchal plate. There are no traces of the posterior pit line and occipital cross-commissure.

Inferognathal

Best preserved in AA.MEM.DS.9 (Figure 3G) but also visible in PIMUZ A/I 5140 and as a partial external mold in the holotype. The bone is rather slender at its biting division and presents a row of at least four, less than 1 mm high, preserved teeth. The jaw is higher in the posterior half, i.e., the bony shaft.

Thoracic armor

In lateral-view, the main part of the thoracic armor of *Amazichthys trinajsticae* has a rectangular and straight appearance with subparallel anterior and posterior edges (Figure 5). Measurements of plate proportions, along with other postcranial elements, are shown in Table 2. The single median dorsal plate is short and broad, square to D-shaped, and has a ventral keel (Figures 5A,C). The posterior margin forms a triangular embayment with an angle of 110 degrees at the tip located nearly halfway from the dorsal and ventral margins. The median dorsal plate presents an angle of 60 degrees at the dorsal margin between the left and right sides. The anterior dorsolateral plate is five-sided, with its posteroventral edge being the smallest, a sixth the length of the posterior margin. The main lateral line passes dorsally on the anterolateral margin to ventrally on the posterior margin and continues to the posterior dorsolateral plate in PIMUZ A/I 4773 but not in AA.MEM.DS.8 nor PIMUZ A/I 5140. The posterior dorsolateral plate is elongate, sub-rectangular, and presents an anteroventral process pointing ventrally. The posterior and ventral margins of the plate are not well-preserved in all specimens. The anterior lateral plate is partially preserved, but its contour is unclear in all specimens with the plate visible and presents a

TABLE 1 Measurements of the skull roof of *Amazichthys trinajsticae* gen. et sp. nov.

	PIMUZ A/I 5141		AA.MEM.DS.8	
	L	W	L	W
Skull roof	119	124	135	129
Pineal	32	18		
Preorbital	28	28		
Central	64	35		
Postorbital	40	25		
Marginal	21	32		
Paranuchal	40 l	34 r		
Nuchal	46	52		
Inferognathal			69	15

Length (L) and width (W) of each best-preserved plate from the skull roof of PIMUZ A/I 5141 and the inferognathal of the holotype AA.MEM.DS.8. Values are in mm. Values in red are approximations due to an unclear margin.

structure resembling a sensory line in both PIMUZ A/I 4773 and PIMUZ A/I 5140 (**Figures 4C,D**). The posterior lateral plate is not discernible. The ventrolateral plates extend much further posteriorly than the median dorsal plate. The same kind of dermal ornamentation as on the skull roof is present on the thoracic armor (**Figures 4C–E**).

Scapulocoracoid

AA.MEM.DS.8 has a circular element resting above the right PVL that may represent a portion of the right scapulocoracoid. It is best preserved in PIMUZ A/I 4773 (left one), AA.MEM.DS.10 (right one), and PIMUZ A/I 5140 (left one) although their preservation is only partial (**Figures 6A–E**). It has five partially preserved basals located posteriorly in PIMUZ A/I 4773 (**Figures 6A–C**). The articular crest is visible on the scapulocoracoid's mid-line along with remnants of radial articulatory facets but further details such as the number of facets of their delimitation are not possible. There are two distinct foramina, one above and one below the mid-line. Their position suggests these are neurovascular foramina. The partial scapulocoracoid of AA.MEM.DS.10 is 71 mm long and 33 mm large and has two partially preserved basals on its margin. It has six foramina divided into two rows, one representing the radial articulatory facets and the other neurovascular foramina. The preserved scapulocoracoid of PIMUZ A/I 5140 is 112 mm long and possibly up to 44 mm high (**Figures 6D,E**). It shows the articular crest with three radial articulatory facets, although there are more that are not preserved. The remains of five basals are discernible.

Pectoral fins

AA.MEM.DS.8 is the only specimen preserving an outline of the pectoral fins (**Figures 7A–C**). They are longer than they are high. The one preserved ventrally is less than twice as large as high and the ventral margin corresponds approximately to the margin of the nodule. The one preserved above the ventrolateral plates is about 2.5 times longer than high.

Dorsal fin

The outline of the dorsal fin is visible in the holotype (**Figure 7D**). The shape of the dorsal fin is partially preserved through the margins of the nodule in PIMUZ A/I 4773 but the dorsal edge is incomplete. Remains of basal fin elements are discernible in AA.MEM.DS.8, A/I 4773, AA.MEM.DS.10, and PIMUZ A/I 5140. They are located dorsally of the neural arches and are preserved as a row of elongate external molds shortly posterior to the dorsal edge of the median dorsal plate. The preservation of contours is quite poor; they are best preserved in PIMUZ A/I 4773 (**Figures 6F,G**), including imprints of 23 ca. 1 mm thick, tubular structures. PIMUZ A/I 5140 has 19 partial basals preserved with only the ventral half remaining but no dorsal fin margin is preserved.

Axial skeleton

In the holotype, a total of 36 remnants of axial skeletal elements, possibly neural arches, are present posterior to the dorsal fin. They are scattered and some are only preserved as slightly lighter colored short rectangular patches. There are putative remains of the neural arches in PIMUZ A/I 4773. The preservation is neither sufficient to distinguish the paraphyses nor articulation between the neural arches.

Pelvic girdle

The imprint of the left mesial side of the pelvic girdle is preserved halfway between the posterior end of the PVL and the anterior end of the "lateral keel" in AA.MEM.DS.8 (**Figures 6H–J**). The basal plate is short and triangular, with a 25-mm-long dorsal iliac process and a posteroventral structure. A total of four preserved radials are attached to the girdle, two shifted by the dorsal margin and two near the anterior end of the basal plate.

Caudal fin

A heterocercal caudal fin is preserved in AA.MEM.DS.8 (**Figure 7F**) and PIMUZ A/I 4773, with a dorsal lobe longer than the ventral one. In the holotype AA.MEM.DS.8, the dorsal lobe is about 220 mm long, tapering distally, where it ends in a rounded lobe. The ventral lobe also has a rounded end but is shorter, 160 mm long.

Remarks

Cranial morphology

The shape of the pineal plate resembles that of *Gymnotrachelus* (Denison, 1978; Carr, 1994; Figures 78B,C) and *Pachyosteus* (Jaekel, 1903; Denison, 1978; Figure 75C), with its "V"-shaped posterior margin. Unlike other selenosteids, the anterior margin of the pineal plate is not positioned dorsal to the

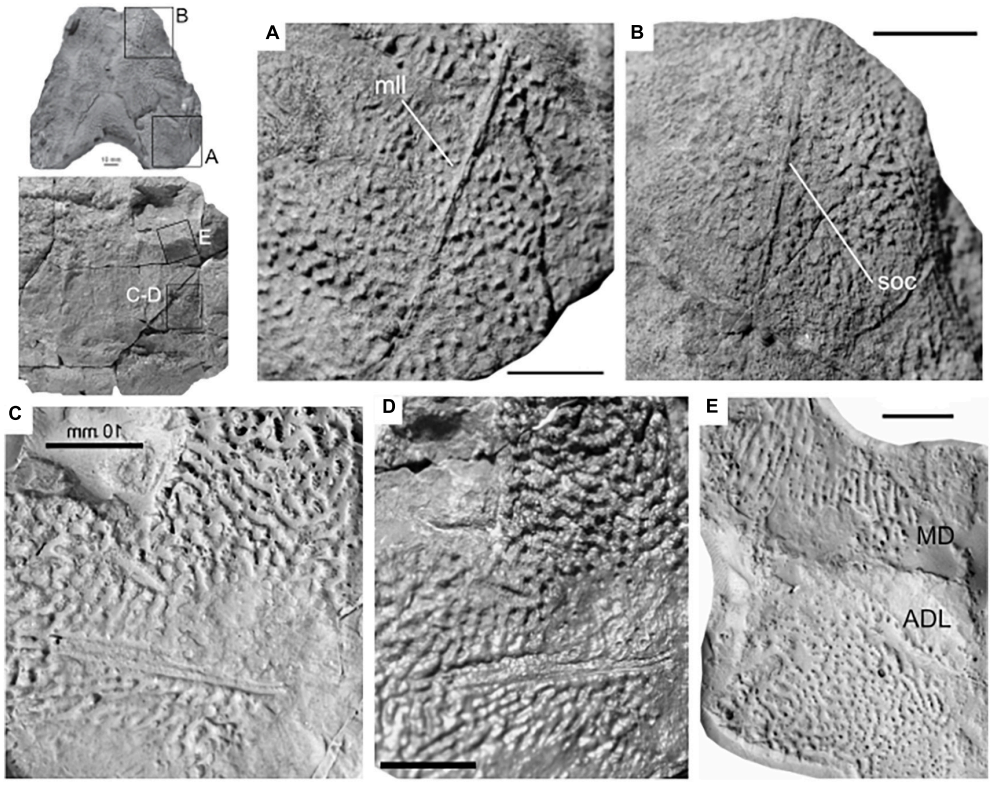

FIGURE 4
Plate ornamentation of *Amazichthys trinajsticae* gen. et sp. nov. Reticular ridges and sensory canals on the paranuchal **(A)**, preorbital **(B)**, anterior lateral **(C),** anterior dorsolateral and median dorsal plates **(D)**. **(A,B)** PIMUZ A/I 5141. Panels **(C,E)** are positives made from the external mold of PIMUZ A/I 4773 **(C–E)**. Scale bars correspond to 10 mm.

orbit, but anterior to it. The preorbital plates are rather similar in shape to those of *Driscollaspis pankowskiorum* (Rücklin et al., 2015). However, the lack of contact between the left and right plates is different for *Driscollaspis*, *Enseosteus* (Jaekel, 1919; Denison, 1978; Figures 75B, 76B; Rücklin, 2011), *Rhinosteus* (Jaekel, 1911; Denison, 1978; Figures 75E, 76A; Rücklin, 2011), *Draconichthys* (Rücklin, 2011), and *Melanosteus* (Lelièvre et al., 1987), and is only seen in *Selenosteus* (Dean, 1901a; Denison, 1978; Figure 78A), *Walterosteus,* and *Gymnotrachelus*. The preorbital plate embayment of the central plate is shallow in *Amazichthys*, as in *Enseosteus* and *Driscollaspis*. The sensory lines form a furrow between elevated bony ridges, which is a feature that has only been documented in *Driscollaspis* so far within the Selenosteidae. The division of the central sensory line into the otic and postorbital branches of the infraorbital canal with a near 45° angle is as seen in *Draconichthys* and *Driscollaspis*. The marginal and central plates are in contact like in *Driscollaspis*, *Melanosteus*, and *Rhinosteus* but the contact is very short relative to other plate contacts in the skull roof as in *Melanosteus*. The paired central plates do not extend posteriorly as a third lobe in the way they do in *Pachyosteus*, *Driscollaspis*, *Rhinosteus,* and *Enseosteus*. The middle pit lines near the center of the central plates of *Amazichthys* are also present in *Rhinosteus* and *Gymnotrachelus* although the position of these pits relative to the skull roof outline is more central in the new genus. The nuchal and paranuchal plates of *Amazichthys* are proportionally as large as the ones of *Driscollaspis* and *Rhinosteus* although they show differences in shape such as smoother paranuchal contact margins with the neighboring plates and different anterior and posterior margins in *Amazichthys*. The paired paranuchal plates do not possess a postnuchal process that surrounds the posterior edges of the nuchal plate. This is a feature that differs from most selenosteids except for the two derived genera *Walterosteus* and *Enseosteus*. The anterior margin of its nuchal plate shows an alternation of small concave and convex curves but as they are minor and balance each other out, this was considered and coded as straight in the character matrix, such as in *Draconichthys*, *Gymnotrachelus,* and *Melanosteus*.

Thoracic armor

The concave posterior dorsal margin of the median dorsal plate is the first record of such shape in the selenosteid family, and more broadly, the arthrodire group. This is likely caused by the position of the dorsal fin and its support structures near the posterodorsal margin of the plate (**Figure 2**). The anterior

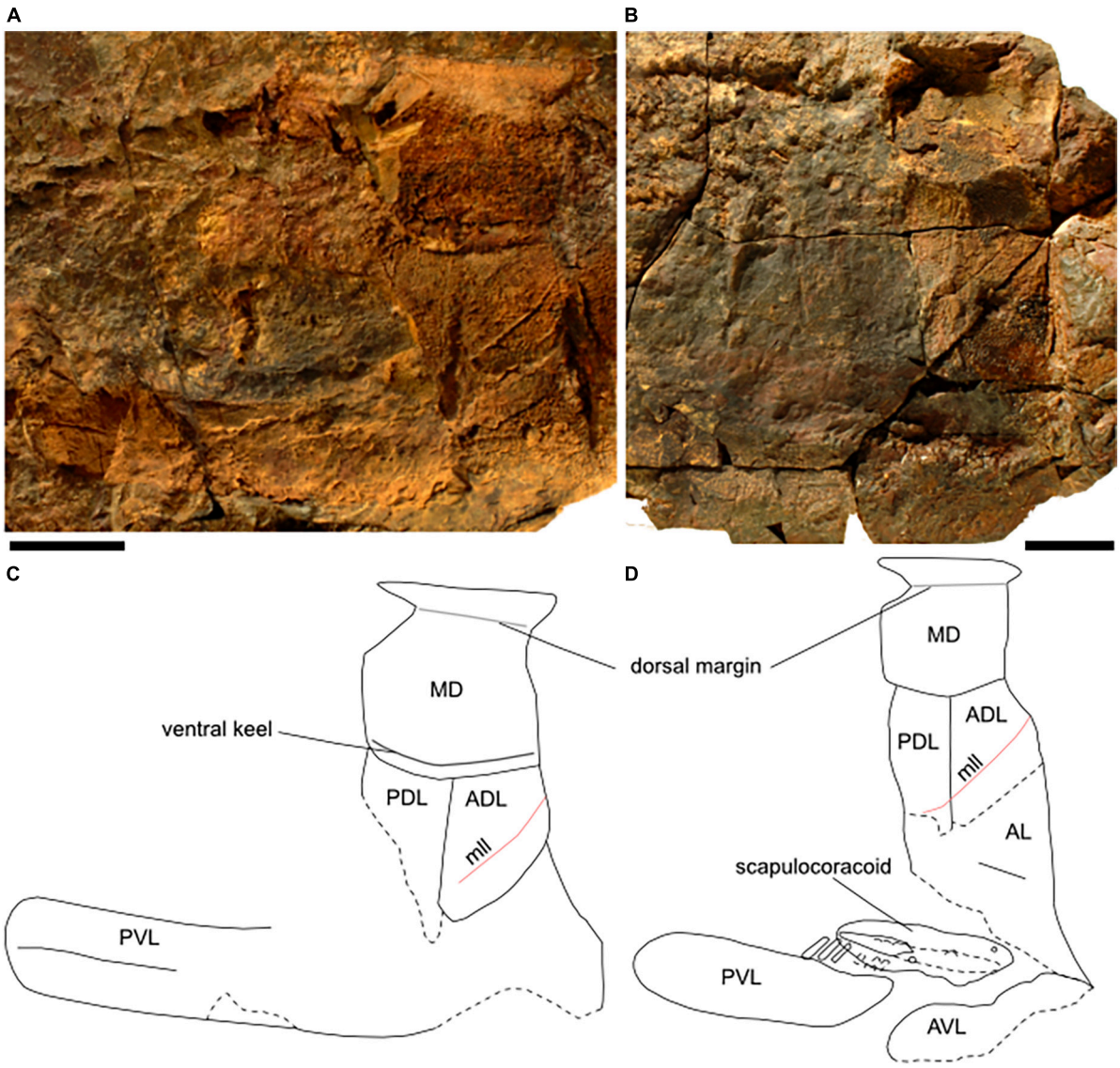

FIGURE 5
Thoracic armor of *Amazichthys trinajsticae* gen. et sp. nov. Thoracic armor of AA.MEM.DS.8, the holotype **(A)**, PIMUZ A/I 4773 **(B)**, and their respective line drawings **(C,D)**. The scale bar corresponds to 50 mm. ADL, anterior dorsolateral plate; AL, anterior lateral plate; AVL, anterior ventrolateral plate; MD, median dorsal plate; PDL, posterior dorsolateral plate; PVL, posterior ventrolateral.

dorsolateral plate of *Amazichthys* is morphologically rather similar to that of *Enseosteus*. Proportionally to the anterior dorsolateral plate, the posterior dorsolateral plate is larger in *Amazichthys* than in other selenosteids where known, the closest in this ratio being *Enseosteus*.

Post-thoracic skeleton

The structures of the axial skeleton in preserved specimens are unclear. The position and orientation of the lower row of shorter tubular structures in PIMUZ A/I 4773 (**Figures 6F,G**) suggest these could be neural arches. The longer tubular structures observed in that same specimen, and similar structures in AA.MEM.DS.8, 10 and PIMUZ 5141, could be other neural arches or basals and radials of the dorsal fin. This is the first selenosteid of which the scapulocoracoid and pelvic girdle are described. As in *Compagopiscis* (Miles and Westoll, 1968) and *Incisoscutum* (Dennis and Miles, 1981; Ahlberg et al., 2009), the scapulocoraoid is rather elongated with the articular crest located centrally. The sub-triangular shape of the pelvic girdle reminds of those of *Coccosteus, Compagopiscis,* and *Incisoscutum*. The ventral margin is rather linear, and the iliac process is elongated, as in *Coccosteus*. Determining with certainty whether this is a left or right girdle is delicate, however, no structures from the lateral

TABLE 2 Measurements of the postcranial elements of *Amazichthys trinajsticae* gen. et sp. nov.

		AA.MEM.DS.8		PIMUZ A/I 4773	
		L	H	L	H
Thoracic armor		181	243	257	217
Median dorsal		80	67	71	63
Anterior dorsolateral		47	49	52	59
Posterior dorsolateral		32	64	27	70
Anterior lateral		–	–	51	95
Anterior ventrolateral		–	–	120	27
Posterior ventrolateral		?	39	143	40
Scapulocoracoid		21	36	98	30
Pelvic girdle	Basal plate	29	29	–	–
	Iliac process	25	5	–	–
	Radials	37	3	–	–
Vertebrae	Near dorsal fin			2–3	28–29
	Near lateral keel			2–3	13
Lateral keel-like structure		211	47	169	40
Dorsal fin		181	88	165	73
Pectoral fin	#1 (most ventral)	120	71	–	–
	#2 (most dorsal)	131	58	–	–
Caudal fin		95 (80[a])	336	88 (59[a])	224
Body		875	257 (339[b])	770	329

Length (L) and height (H) of the thoracic armor and each of its preserved plates, scapulocoracoid, pelvic girdle, vertebrae, structure convergent with a lateral keel, and fins of the holotype AA.MEM.DS.8 and PIMUZ A/I 4773. The width of the caudal fin was taken (under H here) near the base of the tail formation. The body height was taken from the tip of the dorsal fin to the ventral margin of the body. Values are in mm. Values in red are approximations due to an unclear margin. [a]Measured a third from the tip of the lobe. [b]From the tip of the dorsal fin to the tip of the outer pectoral fin.

side of the girdle are visible in this specimen, and look more like a mesial view of the girdle. Thus, we assume that this section is on the left side of the pelvic girdle in mesial view. There is a posteroventral structure that could be interpreted as remnants of the basipterygium in *Amazichthys*. This structure has been observed in the past in *Austrophyllolepis* and *Incisoscutum* (Long et al., 2009) and presents a similar shape to these arthrodires' basipterygium. However, most preserved structures in AA.MEM.DS.8 seem to be from the right side in lateral-view. If the section is on the right side in lateral-view with a poorly preserved surface, the structure may also be interpreted as remnants of the articular crest.

Fins

The dorsal fin is different from what is known from previously described arthrodires, such as *Coccosteus* (Miles and Westoll, 1968) and *Africanaspis* (Gess and Trinajstic, 2017), where it is located more posteriorly. In the latter genera, there appears to be some distance between the posterior margin of the pectoral girdle and the anterior end of the dorsalis. The difference in proportions between the pectoral fins of AA.MEM.DS.8 is likely of taphonomic origin, possibly linked with the angle of embedding, bending, and compaction of the sediment. The caudal fin of PIMUZ A/I 4773 only shows one lobe. The "lateral keel" appears to be oriented slightly differently at its posterior end, possibly indicating that the dorsal lobe flipped downward. This would explain why the seemingly ventral lobe is as long as the dorsal lobe in the better-preserved holotype, suggesting that the dorsal lobe is overlapping with the ventral one. Anterior to the caudal fin is a "lateral keel." This structure is preserved in both specimens with body outline, which suggests this is not a preservation artefact, but rather a lateral thickening of soft tissue.

Discussion

Phylogenetic analysis and systematic position

The phylogeny presented here is based on the emended character matrix by Rücklin et al. (2015). A few minor errors were corrected (list of changes in **Supplementary material**) and *Amazichthys* was added. A new character state was introduced for the character (37), which describes the shape of the posterior

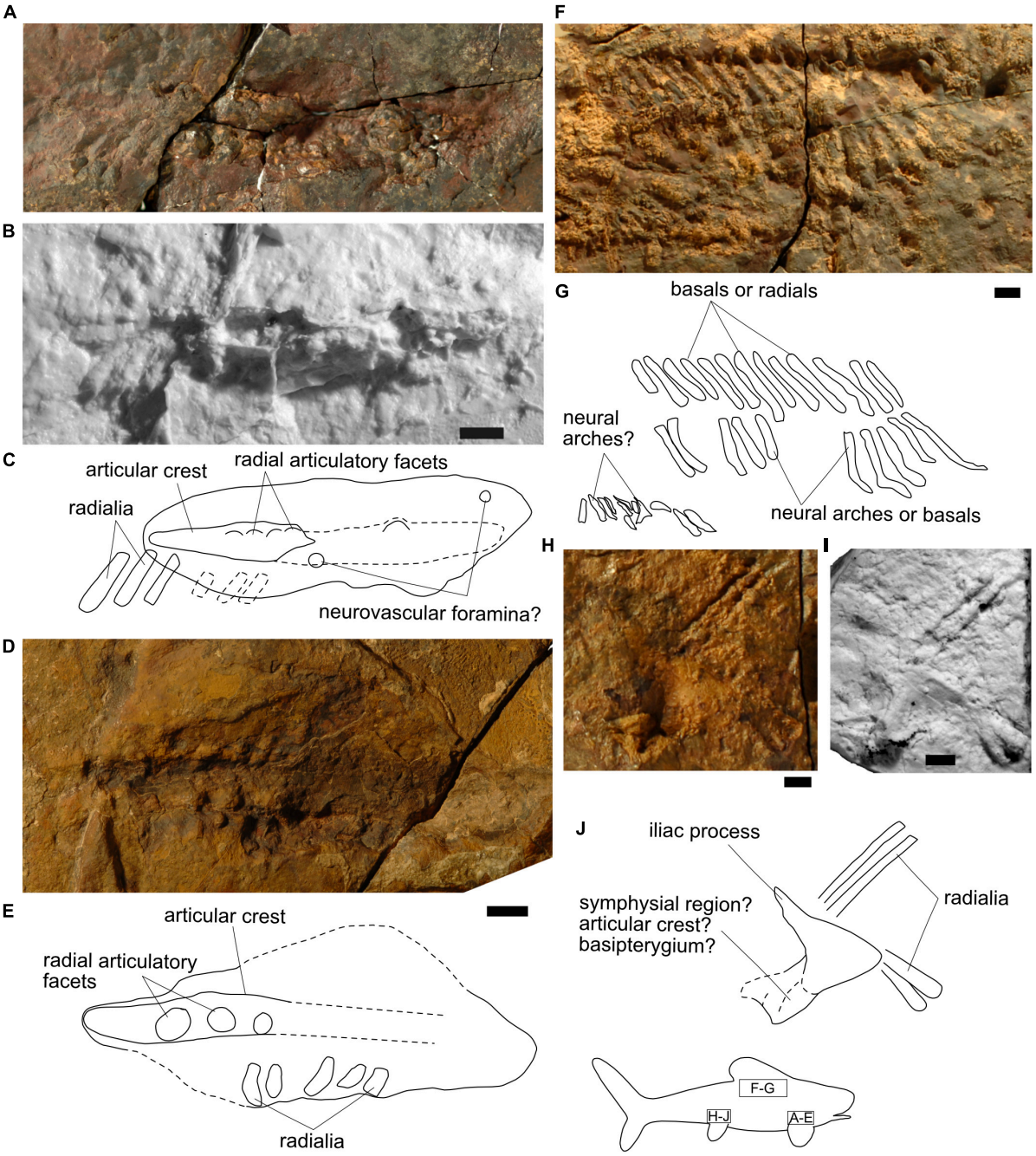

FIGURE 6
Post-thoracic structures of *Amazichthys trinajsticae* gen. et sp. nov. Scapulocoracoid of PIMUZ A/I 4773 **(A–C)** and PIMUZ A/I 5140 **(D,E)**, basals of the dorsal fin in PIMUZ A/I 4773 **(F,G)** and pelvic girdle of AA.MEM.DS.8 **(H–J)**. Scale bars correspond to 10 mm.

end of the median dorsal plate: (0) rounded, (1) spinous or convex, and (2) depressed or concave. Characters 4, 14, 20, 28, 35, 51, 75, 92, and 93 were ordered, and all other characters were unordered. All cladograms are based on a parsimony heuristic search in PAUP with random addition sequence of 10 repetitions and holding 100 trees option. All trees were rooted using the default option "make outgroup paraphyletic." There are four outgroups in the matrix, *Dicksonosteus*, *Holonema*, *Buchanosteus,* and *Homosteus*. The updated character matrix and character list are available in the **Supplementary material**.

The analysis of the new matrix resulted in five trees (**Supplementary material**) with a tree length of 391 steps, CI = 0.350, and RI = 0.546. Both a strict consensus tree and a 50% majority rule consensus tree were computed from the analysis

FIGURE 7
Fins of *Amazichthys trinajsticae* gen. et sp. nov., AA.MEM.DS.8, the holotype. **(A)**, and a close-up in lateral-view of both pectoral fins **(B,C)**, the dorsal fin **(D)**, a structure apparent to a lateral keel **(E)**, and the caudal fin **(F)**. The scale bar corresponds to 100 mm (same scale for **B–E**).

(Figure 8). The majority rule consensus tree (Figure 8A) resolves clade 1, Pachyosteomorphi; clade 2, Aspinothoracidae; clade 3, Selenosteidae; and suggests a solution for unnamed clades 4–8. The strict consensus tree (Figure 8B) results in a polytomy between *Rhinosteus*, *Stenosteus*, *Driscollaspis*, *Selenosteus*, clade 4, and clade 7. Clade 7, which includes *Amazichthys*, *Melanosteus*, *Draconichthys*, *Enseosteus*, and *Walterosteus*, is resolved in both consensus trees.

In the majority rule consensus tree, the monophyly of clade 3, the Selenosteidae family, is supported by large orbits [character 28 (2)], the position of the Pro/Pto/C contact over the orbit [character 33 (1)], the loss of the interolateral branchial lamina [character 47 (0)], and the partially closed angle between the postorbital and otic branches of the infraorbital sensory canal [character 75 (1)]. The presence of a median hypophysial vein foramen is also included [character 73 (1)] as support, but this character is only coded in two selenosteids in the matrix. Clade 3 is possibly resolved in the strict consensus tree but has a polytomy with *Stenosteus*, which sometimes branches as a stem selenosteid in the previously published phylogenies (Rücklin, 2011; Rücklin et al., 2015).

Clade 5 is resolved by a contact of the preorbital plates anterior to the pineal plate [character 18 (1)], a suborbital marginal contact [character 55 (1)], loss of the detent process on

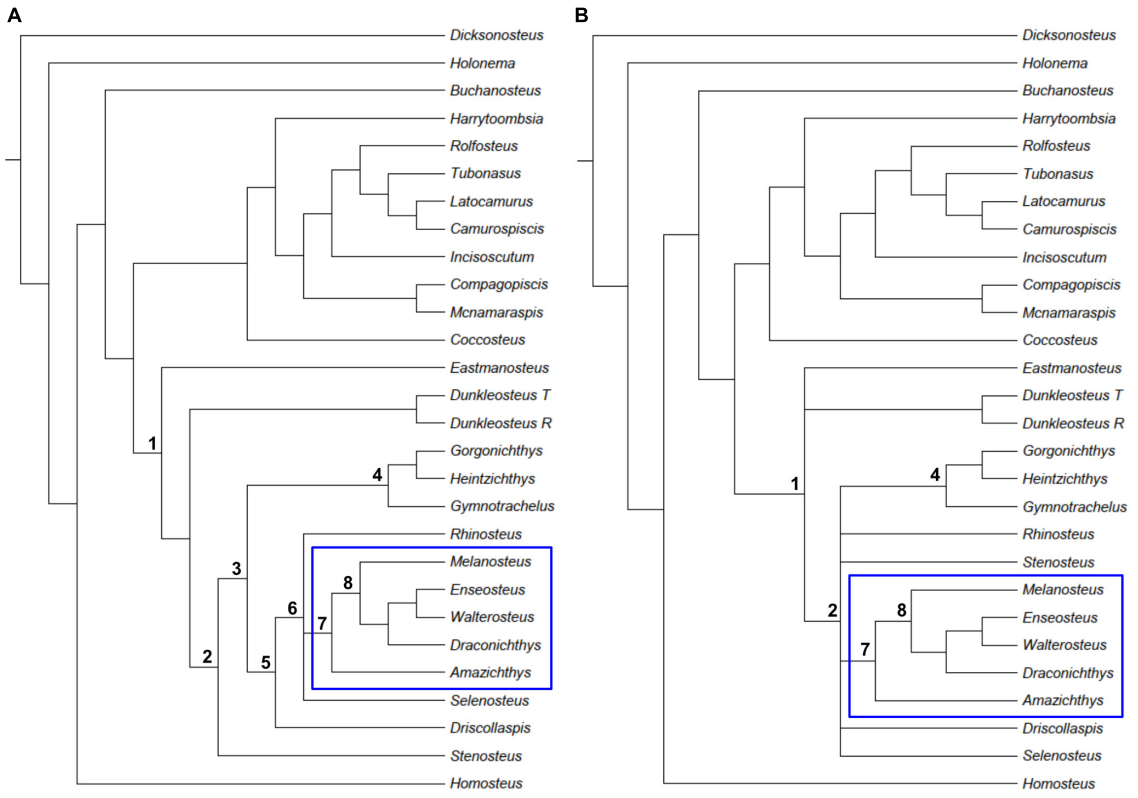

FIGURE 8
Phylogenetic analysis of eubrachythoracid arthrodires and the position of *Amazichthys trinajsticae* gen. et sp. nov. Strict consensus tree **(A)** and majority rule consensus tree **(B)**. Clade 7, in which *A. trinajsticae* is nested, is highlighted by the blue rectangle. 1. Pachyosteomorphi, 2. Aspinothoracidae, 3. Selenosteidae, 4–8. unnamed groups.

the quadrate [character 58 (0) and only coded in *Selenosteus*], and well-bound cheek plates [character 62 (1)]. Additional support is provided by characters 71 (1) and 74 (1) for clade 4, but these are coded equally with another character state and only in two taxa differently, respectively.

Clade 6 is resolved by the external longitudinal lengths of the central plates longer than that of the preorbital plates [character 15 (2)], a long median preorbital plate contact [character 19 (1)], the marginal plate forming part of the orbit [character 25 (1)] and the closed angle between the postorbital and otic branches of the infraorbital sensory canal [character 75 (2)]. Within clade 6, clade 7, *Rhinosteus* and *Selenosteus* are a polytomy.

Clade 7 is resolved in both the strict and majority consensus trees. In the majority consensus tree, it is supported by the straight shape of the external anterior nuchal border [character 10 (0)], the absence of the postnuchal process of the paranuchal plate on the dermal surface [character 30 (0)], a median dorsal plate with a ventral ridge or thickening [character 35 (0)], the presence of a contact between the anterior lateral plate and the anterior ventrolateral plate [character 38 (1)], the absence of a submarginal plate that is closely associated with the hyomandibular [character 59 (0)], the presence of a postorbital sensory line on the suborbital plate [character 81 (1)], the closed angle (<90°) between the postorbital and suborbital branches of the infraorbital sensory line [character 82 (1)], the presence of dermal ornamentation [character 91 (1)] and the position of the posterolateral corner of the skull [character 92 (0)]. The potential movement of the main lateral line onto the posterior dorsolateral plate [character 79 (A)] also provides support; however, it is only coded for *Amazichthys*, *Rhinosteus*, and *Gymnotrachelus* within the entire selenosteid family. In the strict consensus tree, clade 7 is also supported by all the characters cited previously with the addition of a neurocranial thickening [character 4 (1)], central plates longer than the preorbital plates [character 15 (2)], and a long median preorbital plate contact [character 19 (1)]. The parasphenoid prehypophyseal and posthypophyseal shelf widths are shorter than their length [character 71 (1)] and the presence of a parasphenoid ventromedian crest [character 74 (1)] are also supporting the clade but they are coded in three and two selenosteids only, respectively.

Within clade 7, *Amazichthys* is resolved as more stemward to *Melanosteus* and the rest of clade 8 and is supported by five characters in the strict consensus tree: characters 8 (1), 13

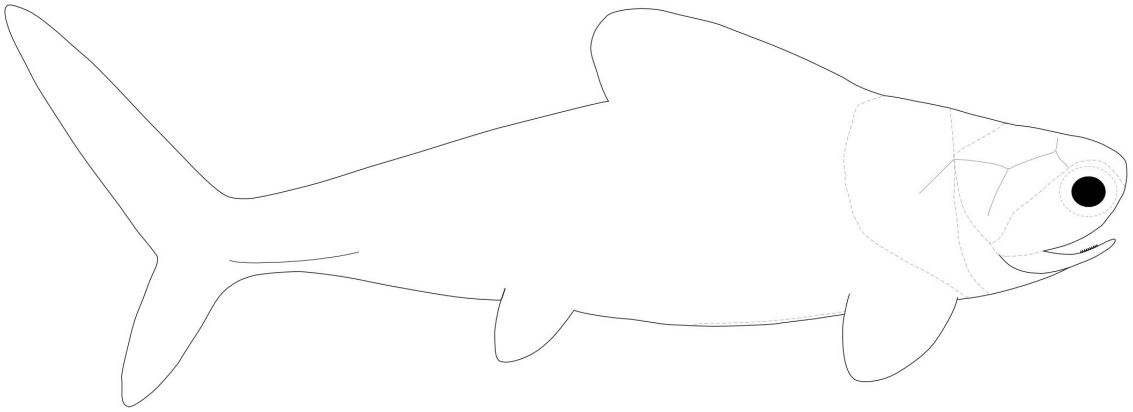

FIGURE 9
Body outline reconstruction of *Amazichthys trinajsticae* gen. et sp. nov. based on the holotype AA.MEM.DS.8, skull roof PIMUZ A/I 5141 and PIMUZ A/I 4773.

(1), 25 (0), 63 (0), and 94 (1). In the majority consensus tree, there are three characters in addition to the ones previously described for node support: 18 (2), 65 (1), and 75 (1). Two additional features are not represented in the matrix and are shared with *Driscollaspis* and ptyctodonts: ornamentation formed by tubular reticular ridges and raised sensory lines. In addition, *Amazichthys* displays a further autapomorphy, namely the sharp concave posterodorsal margin of the median dorsal plate [character 37 (2)], a unique feature within arthrodires.

It is important to note, however, that most selenosteids are rarely complete and thus many of the characters from the thoracic armor, particularly the ventral and posterior plates, are not coded in the majority of selenosteids.

Anatomical reconstruction and ecomorphology

The *Amazichthys* reconstruction (**Figures 9**, **10**) is based on the preserved body outlines of AA.MEM.DS.8 and A/I 4773 as well as the skull roof PIMUZ A/I 5141. The cheekbone area and upper jaws of *Amazichthys* are unknown and, therefore, remain speculative. Pectoral fins present in AA.MEM.DS.8 were subjected to some compression and both fins have different morphologies. However, the right fin, located centrally in the specimen, is more compressed and wider than the left fin, located ventrally. This might be partially due to the weight of the body resting on the fin as it sunk to the seafloor and became compacted with the surrounding sediment. In this reconstruction, the outline of the pectoral fin is a combination of both. The pelvic girdle and its preserved radials were used as a good basis for the reconstruction of the pelvic fin.

Results of the Elliptic Fourier analyses (EFA) show that the morphological variation in the body of sharks can be summarized as changes affecting mainly the body height and the relative size of the caudal fin lobes (**Figure 11**). Thus, PC1 represents changes in the body height, the span of the caudal fin and the degree of development of the caudal fin's ventral lobe; PC2 represents changes in the body height (affecting mostly the ventral margin) and the degree of development of the caudal fin's dorsal lobe; PC3 represents changes in the body height (affecting mostly the dorsal margin) and the angle of the caudal fin's dorsal lobe. PC1, PC2, and PC3 explain the 59, 13, and 6% of the total variance, respectively. The different ecomorphotypes cluster as follows: benthic species in the lowest scores of the PC1, high scores of the PC2, and middle scores of the PC3; bathic and micropelagic in middle to low scores of the PC1 and PC2, and middle scores of the PC3; littoral pelagic species in middle to high scores of the PC1 and PC2, and middle scores of the PC3; and macropelagic species in high scores of the PC1 and PC3 and low scores of the PC2. *Amazichthys* is placed in the highest scores of the PC1, and middle scores of the PC2 and PC3. The analysis of Euclidean distances supports that the body outline of *Amazichthys* is morphologically more similar to those of macropelagic species than to any other ecomorphotype (**Table 3**).

Geometric morphometrics analyses revealed that the morphological variation in the caudal fin of sharks can be summarized as changes affecting the amplitude and relative size of the caudal fin lobes (**Figure 11**). The first two PC axes mirror the results derived from EFA analysis, representing changes in the amplitude of the caudal fin and the degree of development of the caudal fin's ventral lobe (in PC1), and in the degree of development of the caudal fin's dorsal lobe (in PC2). PC3 represents changes in the degree of development of the caudal fin's ventral lobe. PC1, PC2, and PC3 explain the 63, 19, and 8% of the total variance, respectively. The different ecomorphotype clusters are as follows: Benthic species in the middle to high scores of the PC1 and PC3, and middle to low scores of the PC2; bathic and micropelagic in middle to low scores of the

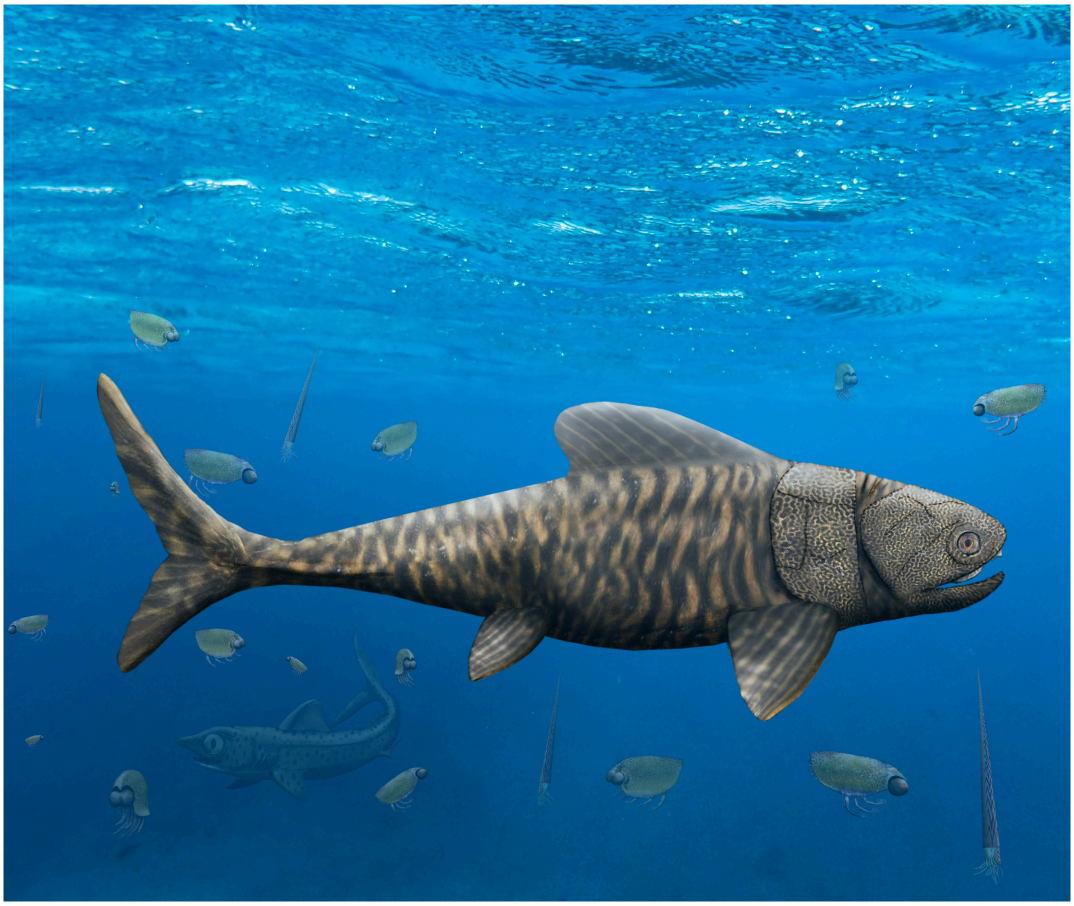

FIGURE 10
Reconstruction of *Amazichthys trinajsticae* gen. et sp. nov.

PC1, PC2, and PC3; littoral pelagic species in middle to low scores of the PC1, and high scores of the PC2 and PC3; and macropelagic species in the lowest scores of the PC1, and middle scores of the PC2 and PC3. *Amazichthys* is placed in the lowest scores of the PC1, and middle scores of the PC2 and PC3. The analysis of Euclidean distances supports that the caudal fin outline of *Amazichthys* is morphologically more similar to those of macropelagic species than to any other ecomorphotype (**Table 3**).

Morphometric analyses on both body and caudal fin outlines of living sharks (with EFA and GM, respectively) reveal a good separation between pre-established ecomorphotypes, in agreement with previous studies (e.g., Ferrón et al., 2017; Sternes and Shimada, 2020). The location of *Amazichthys* within the morphospace derived from the first three PCs suggests that the body and the caudal fin of this placoderm are morphologically very close to those of macropelagic sharks, which is further supported by the Euclidean distances calculated from the whole multidimensional space (**Table 3**). It is worth noting the extreme position of *Amazichthys* in the PC1 of both analyses where this axis represents a gradient toward increasingly pelagic and active lifestyles, with benthic, bathic and micropelagic, litoral pelagic, and macropelagic species gradually distributed from negative to positive scores. In any case, despite being very close, *Amazichthys* does not always fall within the cluster of macropelagic sharks, which might reflect differences inherent to the placoderm body plan, besides the impact of the presence of a caudal fin with an exceptionally large amplitude and well-developed ventral lobe (which might explain the extreme scores of *Amazichthys* within the PC1 derived from the EFA). These results support that *Amazichthys* had a highly active lifestyle most likely as a pelagic cruiser able to maintain high swimming speeds. This is further supported by the (presumed?) presence of caudal lateral keels, a structure that is exclusive to thunniform aquatic vertebrates such as tunas (Zhang et al., 2020), lamnid sharks (Bernal et al., 2001; Donley et al., 2004; Shadwick, 2005), cetaceans (Fish, 1998), and ichthyosaurs (Lingham-Soliar and Plodowski, 2007; Lingham-Soliar, 2016), playing a key role in thrust generation (Zhang et al., 2020). Additionally, the high aspect ratio is

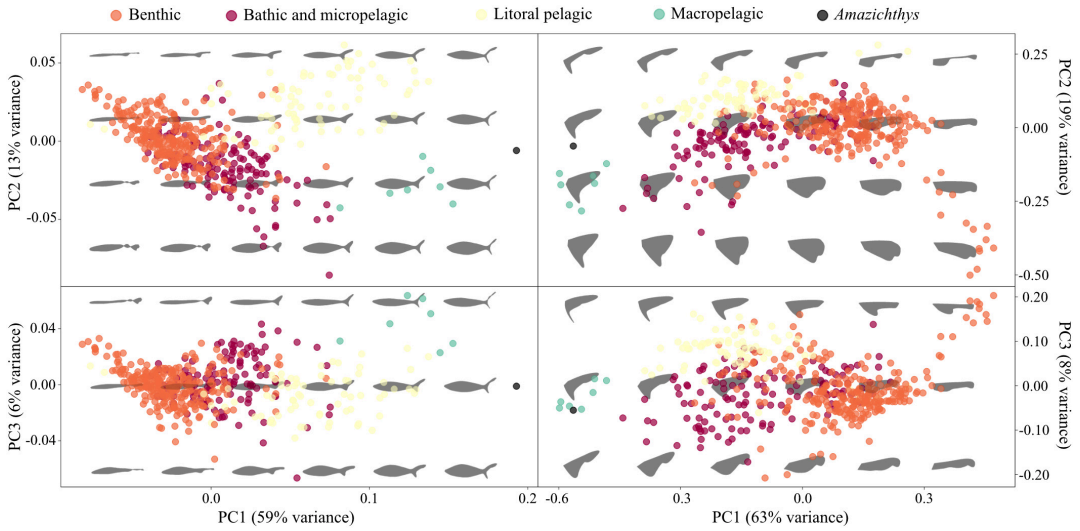

FIGURE 11
Principal Component Analysis (PCA) results for the entire shark group and *Amazichthys trinajsticae* gen. et sp. nov. PCA plots for the first three PC axes show the distribution of ecological morphotypes based on Thomson and Simanek (1977) using the body outline and the caudal fin.

TABLE 3 Euclidean distances between *Amazichthys trinajsticae* gen. et sp. nov. and shark ecomorphotypes calculated after principal component analysis from Elliptical Fourier analyses on the whole body and geometrics morphometrics on the caudal fin.

	Elliptic fourier analysis		Geometric morphometrics	
	Mean	**SD**	**Mean**	**SD**
Benthic	0.22955895	0.021408473	0.703564274	0.130164886
Bathic and micropelagic	0.200466062	0.020608042	0.506220114	0.140578944
Litoral pelagic	0.156868551	0.035520089	0.494326741	0.113165462
Macropelagic	0.099768312	0.022432387	0.240115979	0.039851583

Distances are calculated considering the whole multidimensional space (all PCs).

rather unusual within the placoderm group, where most known caudal fins are also heterocercal but with a low aspect ratio such as the arthrodires *Coccosteus* and *Africanaspis*. A low aspect ratio implies low speeds and a lack of ability to perform bursts of acceleration while a high aspect ratio favors the opposite (Carr, 1995). This implies a broader variety of swimming strategies within the group which was not known before.

Summary

Amazichthys trinajsticae is one of the most complete selenosteids, although many of the bones are preserved as imprints only. It displays a novel feature in the median plate of the thoracic armor, which is unique to the arthrodire group. The exceptional preservation of a body outline on two specimens shows that the dorsal fin was placed near the posterior end of the thoracic armor, which is not the case in the other arthrodires where the dorsalis is known. Additionally, the combination of the caudal fin's high aspect ratio and the presence of a structure apparent to a lateral keel suggests *Amazichthys* was pelagic and capable of reaching and maintaining high-swimming speeds. Rare finds such as body or caudal fin outlines, combined with geometric morphometrics and morphospace visualization and exploration methods, contribute greatly to our understanding of stem-gnathostomes lifestyles. Since the Moroccan fauna yields similar preservation to other placoderms, we expect similar results to be achieved in the near future.

Data availability statement

The original contributions presented in the study are included in the article/**Supplementary material**, further inquiries can be directed to the corresponding author. The taxonomic data can be found at https://zoobank.org/NomenclaturalActs/b8043f7d-94f8-4bfe-bb82-71cff88147ef and https://zoobank.org/NomenclaturalActs/58387be0-45d0-4b75-8b4f-5c75f8ef49e7.

Ethics statement

Ethical review and approval was not required for the animal study because it presents results for fossil vertebrates only.

Author contributions

MJ and CK had the idea and designed the study. MJ described the specimens and produced most of the figures. HF performed the ecomorphology analysis. MJ and MR produced the additional data for the character matrix and performed the phylogenetic analysis. All authors contributed to the figures, wrote parts of the text, proofread various versions of the text, and approved the final version of the manuscript.

Funding

MJ and CK were funded by the Swiss National Science Foundation (project no. 200020_184894).

Acknowledgments

Saïd Oukherbouch (Tafraoute) discovered the specimens from the Maïder while Mohamed Mezane (La Khraouia) collected the specimens from the Tafilalt. Merle Greif and Beat Scheffold (both Zürich) made silicon casts of different structures. We thank Aldo Benites Palomino (Zürich) for his insight and advice on the phylogenetic analysis. Stephan Spiekman (Stuttgart) segmented AA.MEM.DS.11. The Ministère de l'Energie, des Mines, de l'Eau et de l'Environnement (Direction du Développement Minier, Division du Patrimoine, Rabat, Morocco) provided work and sample export permits. We also thank the reviewers and the editor for their input.

Conflict of interest

The authors declare that the research was conducted in the absence of any commercial or financial relationships that could be construed as a potential conflict of interest.

Publisher's note

Supplementary material

The Supplementary Material for this article can be found online at: https://www.frontiersin.org/articles/10.3389/fevo.2022.969158/full#supplementary-material

References

Adams, D. C., Collyer, M., Kaliontzopoulou, A., and Sherratt, E. (2016). *Geomorph: Software for geometric morphometric analyses*. New York: R core Team.

Ahlberg, P., Trinajstic, K., Johanson, Z., and Long, J. (2009). Pelvic claspers confirm chondrichthyan-like internal fertilization in arthrodires. *Nature* 460, 888–889. doi: 10.1038/nature08176

Anderson, P., Friedman, M., Brazeau, M., and Rayfield, E. (2011). Initial radiation of jaws demonstrated stability despite faunal and environmental change. *Nature* 476, 206–209. doi: 10.1038/nature10207

Becker, R. T., House, M. R., Bockwinkel, J., Ebbighausen, V. and Aboussalam, Z. S. (2002). Famennian ammonoid zones of the eastern Anti-Atlas (southern Morocco). *Münster. Forsch. Geol. Paläont.* 93, 195–205.

Bernal, D., Dickson, K., Shadwick, R., and Graham, J. (2001). Review: Analysis of the evolutionary convergence for high performance swimming in lamnid sharks and tunas. *Comp. Biochem. and Physiol. Part A* 129, 695–726. doi: 10.1016/S1095-6433(01)00333-6

Bonhomme, V., Picq, S., Gaucherel, C., and Claude, J. (2014). Momocs: Outline Analysis Using R. *J. Statist. Softw.* 56, 1–24. doi: 10.18637/jss.v056.i13

Brazeau, M. D., and Friedman, M. (2014). The characters of Palaeozoic jawed vertebrates. *Zool. J. Linn. Soc.* 170, 779–821. doi: 10.1111/zoj12111

Brazeau, M. D., and Friedman, M. (2015). The origin and early phylogenetic history of jawed vertebrates. *Nature* 520, 490–497. doi: 10.1038/nature14438

Carr, R. K. (1994). *A redescription of Gymnotrachelus (Placodermi: Arthrodira) from the Cleveland Shale (Famennian) of Northern Ohio, U.S.A.* Cleveland: Cleveland Museum of Natural History.

Carr, R. K. (1995). Placoderm diversity and evolution. *Bull. Muséum Natl. Nat.* 17, 85–125.

Carr, R. K., Johanson, Z., and Ritchie, A. (2009). The Phyllolepid Placoderm *Cowralepis mclachlani*: Insights into the Evolution of Feeding Mechanisms in Jawed Vertebrates. *J. Morpho.* 270, 775–804. doi: 10.1002/jmor.10719

Carr, R. K., Lelievre, H., and Jackson, G. (2010). "The ancestral morphotype for the gnathostome pectoral fin revisited and the placoderm condition," in *Phylogeny and Paleobiogeography of Fossil Fishes*, eds D. K. Elliott, J. G. Maisey, X. Yu, and D. Miao (New Delhi: Morphology), 107–122.

Coatham, S. J., Vinther, J., Rayfield, E. J., and Klug, C. (2020). Was the Devonian placoderm Titanichthys a suspension feeder? *Roy. Soc. Open Sci.* 7:200272. doi: 10.1098/rsos.200272

Dean, B. (1901a). Palaeontological Notes. I. On two new arthrodires from the Cleveland Shale of Ohio. *Mem. New York Acad. Sci.* 2, 87–100.

Dean, B. (1901b). Palaeontological Notes. III. Further notes on the relationships of the Arthrognathi. *Mem. New York Acad. Sci.* 2, 110–123.

Denison, R. (1978). *Handbook of paleoichthyology Volume 2. Placodermi*. Fischer: Stuttgart.

Dennis, K., and Miles, R. S. (1981). A pachyosteomorph arthrodire from Gogo, Western Australia. *Zool. J. Linn. Soc.* 73, 213–258. doi: 10.1111/j.1096-3642.1981.tb01594.x

Donley, J. M., Sepulveda, C. A., Konstantinidis, P., Gemballa, S., and Shadwick, R. E. (2004). Convergent evolution in mechanical design of lamnid sharks and tunas. *Nature* 429, 61–65. doi: 10.1038/nature02435

Donoghue, P. C., Forey, P. L., and Aldridge, R. J. (2000). Conodont affinity and chordate phylogeny. *Biol. Rev. Camb. Philos. Soc.* 75, 191–251. doi: 10.1017/S0006323199005472

Ebert, D. A., Fowler, S. L., Compagno, L. J. V., and Dando, M. (2013). *Sharks of the world : a fully illustrated guide*. Plympton St. Maurice: Plymouth Wild Nature Press.

Ferrón, H. G., Martínez-Pérez, C., and Botella, H. (2017). Ecomorphological inferences in early vertebrates: reconstructing Dunkleosteus terrelli (Arthrodira, Placodermi) caudal fin from palaeoecological data. *PeerJ* 5:e4081. doi: 10.7717/peerj.4081

Fish, F. E. (1998). Comparative kinematics and hydrodynamics of odontocete cetaceans: Morphological and ecological correlates with swimming performance. *J. Exp. Biol.* 201, 2867–2877. doi: 10.1242/jeb.201.20.2867

Forey, P. L., and Janvier, P. (1993). Agnathans and the origin of jawed vertebrates. *Nature* 361, 129–134. doi: 10.1038/361129a0

Frey, L., Coates, M., Ginter, M., Hairapetian, V., Rücklin, M., Jerjen, I., et al. (2019a). The early elasmobranch Phoebodus: phylogenetic relationships, ecomorphology and a new time-scale for shark evolution. *Proc. Roy. Soc. B* 286:20191336. doi: 10.1098/rspb.2019.1336

Frey, L., Pohle, A., Rücklin, M., and Klug, C. (2019b). Fossil-Lagerstaütten, palaeoecology and preservation of vertebrates and invertebrates from the Devonian of Morocco (eastern Anti-Atlas). *Lethaia* 53, 242–266. doi: 10.1111/let.12354

Frey, L., Coates, M. I., Tietjen, K., Rücklin, M., and Klug, C. (2020). A symmoriiform from the Late Devonian of Morocco demonstrates a derived jaw function in ancient chondrichthyans. *Comm. Biol.* 3, 1–10. doi: 10.1038/s42003-020-01394-2

Frey, L., Rücklin, M., Korn, D., and Klug, C. (2018). Late Devonian and Early Carboniferous alpha diversity, ecospace occupation, vertebrate assemblages and bio-events of southeastern Morocco. *Palaeogeogr. palaeocl. palaeoecol.* 496, 1–17. doi: 10.1016/j.palaeo.2017.12.028

Gardiner, B. G. (1984). The relationships of placoderms. *J. Vert. Paleontol.* 4, 375–395. doi: 10.1080/02724634.1984.10012017

Gess, R. W., and Trinajstic, K. M. (2017). New morphological information on, and species of placoderm fish Africanaspis (Arthrodira, Placodermi) from the Late Devonian of South Africa. *PLoS One* 12, e0173169. doi: 10.1371/journal.pone.0173169

Giles, S., Friedman, M., and Brazeau, M. D. (2015). Osteichthyan-like cranial conditions in an Early Devonian stem gnathostome. *Nature* 520:7545. doi: 10.1038/nature14065

Gross, W. (1961). Lunaspis broilii und Lunaspis heroldi aus dem Hunsrückschiefer (Unterdevon, Rheinland). Notizbl. Hess. Landes. Bodenforsch. *Wiesbaden* 89, 17–14.

Jaekel, O. M. J. (1903). Über die Organisation und systematische Stellung der Asterolepiden. Z. Deutschen Geol. *Gesellschaft* 55, 41–60.

Jaekel, O. M. J. (1911). *Die Wirbeltiere. Gebrüder Bornträger*. Berlin: Verlag Gebrüder Borntraeger.

Jaekel, O. M. J. (1919). *Die Mundbildung der Placodermen. Sitzungsberichte der Gesellschaft Naturforschender Freunde Berlin*. Berlin: Verlag Gebrüder Borntraeger, 73–110.

Janvier, P. (1984). The relationships of the Osteostraci and Galeaspida. *J. Vertebr. Paleontol.* 4, 344–358. doi: 10.1080/02724634.1984.10012014

Jarvik, E. (1980). *Basic structure and evolution of vertebrates*. London: Academic Press.

Jobbins, M., Haug, C., and Klug, C. (2020). First African thylacocephalans from the Famennian of Morocco and their role in Late Devonian food webs. *Sci. Rep.* 10:5129. doi: 10.1038/s41598-020-61770-0

Jobbins, M. E. M., Rücklin, M., Argyriou, T., and Klug, C. (2021). A large Middle Devonian eubrachythoracid 'placoderm' (Arthrodira) jaw from northern Gondwana. *Swiss J. Palaeo.* 140, 1–17. doi: 10.1186/s13358-020-00212-w

Johanson, Z. (1997). New Remigolepis (Placodermi; Antiarchi) from Canowindra, New South Wales, Australia. *Geol. Mag.* 134, 813–846. doi: 10.1017/S0016756897007838

King, B., Qiao, T., Lee, M. S. Y., Zhu, M., and Long, J. A. (2017). Bayesian Morphological Clock Methods Resurrect Placoderm Monophyly and Reveal Rapid Early Evolution in Jawed Vertebrates. *Syst Biol.* 66, 499–516. doi: 10.1093/sysbio/syw107

Klug, C., Di Silvestro, G., Hoffmann, R., Schweigert, G., Fuchs, D., Clements, T., et al. (2021). Diagenetic phosphatic Liesegang rings deceptively resemble chromatophores in Mesozoic coleoids. *PeerJ* 9:e10703. doi: 10.7717/peerj.10703

Kuratani, S. (2012). Evolution of the vertebrate jaw from developmental perspectives. *Evol. Dev.* 14, 76–92. doi: 10.1111/j.1525-142X.2011.00523.x

Lelièvre, H., Feist, R., Goujet, D., and Blieck, A. (1987). Les vertébrés de la Montagne Noire (Sud de la France) et leur apport à la phylogénie des Pachyostéomorphes (Placodermes, Arthrodires). *Palaeovertebrata* 17, 1–26.

Lindgren, J., Sjövall, P., Thiel, V., Zheng, W., Ito, S., Wakamatsu, K., et al. (2018). Soft-tissue evidence for homeothermy and crypsis in a Jurassic ichthyosaur. *Nature* 564, 359–365. doi: 10.1038/s41586-018-0775-x

Lingham-Soliar, T. (2016). Convergence in thunniform anatomy in lamnid sharks and Jurassic ichthyosaurs. *Integr. Comp. Biol.* 56, 1323–1336. doi: 10.1093/icb/icw125

Lingham-Soliar, T., and Plodowski, G. (2007). Taphonomic evidence for high-speed adapted fins in thunniform ichthyosaurs. *Naturwissenschaften* 94, 65–70. doi: 10.1007/s00114-006-0160-8

Long, J., Trinajstic, K., Young, G., and Senden, T. (2008). Live birth in the Devonian period. *Nature* 453, 650–652. doi: 10.1038/nature06966

Long, J. A. (1983). New Bothriolepid fish from the Late Devonian of Victoria, Australia. *Palaeontol* 26, 395–320.

Long, J. A., Mark-Kurik, E., Johanson, Z., Lee, M. S. Y., Young, G. C., and Min, Z. (2015). Copulation in antiarch placoderms and the origin of gnathostome internal fertilization. *Nature* 517, 196–199. doi: 10.1038/nature13825

Long, J. A., Trinajstic, K., and Johanson, Z. (2009). Devonian arthrodire embryos and the origin of internal fertilization in vertebrates. *Nature* 457, 1124–1127. doi: 10.1038/nature07732

Maddison, W. P., and Maddison, D. R. (2021). *Mesquite: a modular system for evolutionary analysis. Version 3.70*. Available online at: http://www.mesquiteproject.org (accessed April 8, 2022).

Miles, R. S., and Westoll, T. S. (1968). IX.—The Placoderm Fish Coccosteus cuspidatus Miller ex Agassiz from the Middle Old Red Sandstone of Scotland. Part I. Descriptive Morphology. *T. Roy. Soc. Edin.* 67, 373–476. doi: 10.1017/S0080456800024078

Ørvig, T. (1960). New Finds of Acanthodians, Arthrodires, Crossopterygians, Ganoids and Dipnoans in the Upper Middle Devonian Calcareous Flags (Oberer Plattenkalk) of the Bergisch Gladbach-Paffrath Trough. *Paläontologische Zeitschrift* 34, 295–335. doi: 10.1007/BF02986872

Philippe, J. (1996). *Early vertebrates*. Oxford: Clarendon Press.

R Core Team (2020). *R: A Language and Environment for Statistical Computing*. Vienna: R Foundation for Statistical Computing.

Reif, W. E. (1982). Evolution of dermal skeleton and dentition in vertebrates. *Evol. Biol.* 15, 287–368. doi: 10.1007/978-1-4615-6968-8_7

Rohlf, J. (2016). *tpsDig2. v 2.26*. New York: Stony Brook University, 523.

Rücklin, M. (2011). First selenosteid placoderms from the eastern Anti-Atlas of Morocco; osteology, phylogeny and palaeogeographical implications. *Palaeontol* 54, 25–62. doi: 10.1111/j.1475-4983.2010.01026.x

Rücklin, M., Donoghue, P. C. J., Cunningham, J. A., Marone, F., and Stampanoni, M. (2014). Developmental paleobiology of the vertebrate skeleton. *J. Paleontol.* 88, 676–683. doi: 10.1666/13-107

Rücklin, M., Donoghue, P. C. J., Johanson, Z., Trinajstic, K., Marone, F., and Stampanoni, M. (2012). Development of teeth and jaws in the earliest jawed vertebrates. *Nature* 491, 748–751. doi: 10.1038/nature11555

Rücklin, M., Lelièvre, H., and Klug, C. (2018). Placodermi from the Early Devonian Kess-Kess Mounds of Hamar Laghdad, Southern Morocco. *Neues Jahrbuch für Geologie und Paläontologie, Abhandlungen* 290, 301–306. doi: 10.1127/njgpa/2018/0780

Rücklin, M., Long, J. A., and Trinajstic, K. (2015). A new selenosteid arthrodire ('Placodermi') from the Late Devonian of Morocco. *J. Vert. Paleontol.* 35, 1–13. doi: 10.1080/02724634.2014.908896

Sansom, I. J., Wang, N. Z., and Smith, M. (2005). The histology and affinities of sinacanthid fishes: primitive gnathostomes from the Silurian of China. *Zool. J. Linn. Soc.* 144, 379–386. doi: 10.1111/j.1096-3642.2005.00171.x

Shadwick, R. (2005). How tunas and lamnid sharks swim: An evolutionary convergence. *Am. Sci.* 93, 524–531. doi: 10.1511/2005.56.524

Smith, M. M., and Johanson, Z. (2003). Separate evolutionary origins of teeth from evidence in fossil jawed vertebrates. *Science* 299, 1235–1236. doi: 10.1126/science.1079623

Sternes, P. C., and Shimada, K. (2020). Body forms in sharks (Chondrichthyes: Elasmobranchii) and their functional, ecological, and evolutionary implications. *Zoology* 140:125799. doi: 10.1016/j.zool.2020.125799

Swofford, D. A. (2003). *PAUP* 4.0*. Sunderland: Sinauer Associates.

Thomson, K. S., and Simanek, D. E. (1977). Body Form and Locomotion in Sharks. *Am. Zool.* 17, 343–354. doi: 10.1093/icb/17.2.343

Trinajstic, K., Boisvert, C., Long, J., Maksimenko, A., and Johanson, Z. (2015). Pelvic and reproductive structures in placoderms (stem gnathostomes). *Biol. Rev.* 90, 468–501. doi: 10.1111/brv.12118

Trinajstic, K., Long, J., Sanchez, S., Boisvert, C., Snitting, D., and Tafforeau, P. (2022). Exceptional preservation of organs in Devonian placoderms from the Gogo lagerstätte. *Science* 377, 1311–1314. doi: 10.1126/science.abf3289

Vaškaninová, V., Chen, D., Tafforeau, P., Johanson, Z., Ekrt, B., Blom, H., et al. (2020). Marginal dentition and multiple dermal jawbones as the ancestral condition of jawed vertebrates. *Science* 369, 211–216. doi: 10.1126/science.aaz9431

Wendt, J. (1985). Disintegration of the continental margin of northwestern Gondwana: Late Devonian of the eastern Anti-Atlas (Morocco). *Geology* 13, 815–818. doi: 10.1130/0091-7613(1985)13<815:DOTCMO>2.0.CO;2

Wendt, J. (1988). "Facies pattern and palaeogeography of the Middle and Late Devonian in the eastern Anti-Atlas (Morocco)," in *Devonian of the World, I*, eds N. J. Mc Millan, A. F. Embry, and D. J. Glass (Canada: Canadian Society of Petroleum Geologists), 467–480.

Wendt, J. (2021). Middle and Late Devonian paleogeography of the eastern Anti-Atlas (Morocco). *Int. J. Earth Sci.* 110, 1531–1544. doi: 10.1007/s00531-021-02028-6

Wickham, H. (2016). *ggplot2: elegant graphics for data analysis*. Germany: Springer. doi: 10.1007/978-3-319-24277-4

Young, G. C. (1986). The relationships of the placoderm fishes. *Zool. J. Linn. Soc.* 88, 1–57. doi: 10.1111/j.1096-3642.1986.tb00876.x

Young, G. C. (2010). Placoderms (armoured fish): dominant vertebrates of the Devonian period. *Annu. Rev. Earth Planet. Sci.* 38, 523–550. doi: 10.1146/annurev-earth-040809-152507

Zhang, J. D., Sung, H. J., and Huang, W. X. (2020). Specialization of tuna: A numerical study on the function of caudal keels. *Physic. Fluids* 32:111902. doi: 10.1063/5.0029340

Zhu, M., Ahlberg, P. E., Pan, Z., Zhu, Y., Qiao, T., Zhao, W., et al. (2016). A Silurian maxillate placoderm illuminates jaw evolution. *Science* 354, 334–336. doi: 10.1126/science.aah3764

Zhu, M., Yu, X., Ahlberg, P. E., Choo, B., Lu, J., Qiao, T., et al. (2013). A Silurian placoderm with osteichthyan-like marginal jaw bones. *Nature* 502, 188–193. doi: 10.1038/nature12617

Zhu, Y., Giles, S., Young, G. C., Hu, Y., Bazzi, M., Ahlberg, P. E., et al. (2021). Endocast and Bony Labyrinth of a Devonian 'Placoderm' Challenges Stem Gnathostome Phylogeny. *Curr. Biol* 31, 1112–1118.e4. doi: 10.1016/j.cub.2020.12.046